Compact 4-Port MIMO Antenna-Diplexer Utilizing Slotted-HMSIW Technology

Divya Chaturvedi, *Senior Member, IEEE*, Tiru Ganesh Lanka, *Student Member, IEEE*, and Arvind Kumar, *Senior Member, IEEE*

***Abstract*—A new design for a 4-port multiple input multiple output (MIMO) self-diplexing antenna is introduced, utilizing half-mode substrate integrated waveguide (HMSIW) technology. This antenna operates simultaneously at 4.9 GHz for WLAN and 5.8 GHz for ISM band communications, maintaining an isolation of approximately 30 dB. By employing the half-mode topology, the antenna size is reduced by 50% while preserving the dominant mode TE_{110} characteristics. To enhance bandwidth, a rectangular slot is etched at the centre of each cavity, splitting the dominant mode into odd-TE_{110} and even-TE_{110} modes. Through careful optimization of antenna parameters and the perpendicular placement of radiating elements for different frequencies, the design ensures self-diplexing property. To validate the design, a prototype of the antenna is manufactured, and experimental results are verified with simulations. The proposed antenna demonstrates a peak gain of 5.2 dBi in the lower-frequency band and 5.9 dBi in the upper-frequency band, with a high efficiency exceeding 94% in both of the frequency bands. Additionally, all MIMO-diversity parameters were found to be within satisfactory limits.**

Link to graphical and video abstracts, and to code: https://latamt.ieeer9.org/index.php/transactions/article/view/9679

***Index Terms*— Cavity-backed slot antenna; MIMO; Isolation; antenna-diplexer; substrate integrated waveguide (SIW).**

I. Introduction

In recent years, multi-band antennas have largely been employed in the current wireless compact handheld and mobile devices and systems. To utilize these devices for different applications, they are usually provided with two or more transceivers that can work simultaneously [1]–[2]. The diplexer elements are generally used to provide adequate isolation between the transceiver system's channels. In the last decade, the concept of self-diplexing antenna has become fancy, as it supports self-diplexing ability without using any complex diplexer elements, leading to the simplicity of overall design [3].

In wireless communication, multi-path propagation of carrier-modulated signals often leads to challenges such as fading and co-channel interference, causing significant power loss over long-distances. Enhancing channel capacity is essential for improving performance in dynamic environments, enabling wide-area coverage and high quality of services [4]–[8]. The multi-input multi-output (MIMO) antennas with spatial diversity offer an effective solution by establishing reliable communication links and significantly increasing data throughput. However, designing a compact 4-element MIMO antenna with high isolation remains a complex challenge. Researchers have explored various techniques to improve isolation between elements. In [9], radiating elements were placed on opposite sides of the plane for millimeter-wave 5G communication, achieving a port isolation of 30 dB. In [10], orthogonally placed PIFA-radiating elements with increased separation resulted in 17 dB isolation. Dipole antennas arranged in an orthogonal configuration [11] also showed improved isolation. The inclusion of a T-shaped slot impedance transformer at the antenna edges [12] enhanced isolation by 8 dB, but required a bulky dual-dielectric structure with an air gap, making it non-planar.

To further enhance isolation, a double-layer mushroom metamaterial wall was employed between SIW cavities in a 4-element MIMO antenna [13], achieving 40 dB isolation. However, its 20.8 mm height mushroom metamaterial wall added significant bulk, making it suitable only for applications prioritizing isolation over compactness. Additionally, a ceramic superstrate was used to suppress cross-polarization [14], but this approach increased design complexity due to its multi-layered structure.

Substrate Integrated Waveguide (SIW) technology has emerged as a promising solution for realizing planar, high-isolation MIMO antennas while maintaining structural simplicity. The placement of electric walls in SIW cavities naturally provides intrinsic isolation. Moreover, Half-Mode (HM) SIW and Quarter-Mode (QM) SIW reduce antenna size by 50% and 75%, respectively, without compromising

The associate editor coordinating the review of this manuscript and approving it for publication was Roberto S. Murphy (*Corresponding author: Arvind Kumar*).

D. Chaturvedi is with Dept. of Electronics and Communication Engineering, Indian Institute of Information Technology, Pune, India (e-mail: divya@iiitp.ac.in).

Tiruganesh Lanka is with Dept. of Electronics and Communication Engineering, University-AP, India (e-mail: tiruganesh_l@srmap.edu.in).

A. Kumar is with the Dept. of Electronics and Communication Engineering, Visvesvaraya National Institute of Technology, Nagpur, India (e-mail: arvindkumar@ece.vnit.ac.in).

performance. A 4-element HMSIW cavity-backed self-diplexing antenna [15] demonstrated mutual coupling level, -20 dB further reduced to -30 dB using neutralization lines [16]. In [17], a QMSIW-based dual-band textile MIMO antenna utilized different element orientations to achieve 30 dB isolation, while in [18], a 4-element QMSIW MIMO antenna divided an HMSIW cavity into two QMSIW cavities, improving compactness but limiting isolation less than 20 dB. Another approach in [19] employed shielded HMSIW cavity-backed antennas, where same-frequency elements were placed orthogonally and separated by frog-anatomy slots, achieving 21 dB isolation but offering a narrow 2.2% fractional bandwidth. Despite these advancements, achieving compactness, high isolation, and wide bandwidth in a single-layered MIMO antenna remains a significant research challenge. The proposed antenna provides a solution for compact-size with moderate gain, enhanced interelement isolation, and improved bandwidth.

This work presents a novel and miniaturized 2×2 MIMO antenna-diplexer utilizing Half-Mode Substrate Integrated Waveguide (HMSIW) technology. By leveraging the half-mode SIW concept, the antenna's size is effectively reduced by 50% as compared to full-mode (FM) SIW cavity with maintaining similar features. Additionally, bandwidth is significantly enhanced through the incorporation of an open-ended rectangular slot at the center of each half-mode cavity. This slot bisects the HMSIW cavity into two symmetrical halves, splitting the dominant mode into odd- and even-TE_{110} modes. The proposed antenna achieves a minimum isolation of 30 dB for both orthogonal and parallel elements in a MIMO configuration. Furthermore, it integrates a self-diplexing feature within a single-layered structure, ensuring a compact, low-profile design that facilitates seamless integration into handheld communication devices.

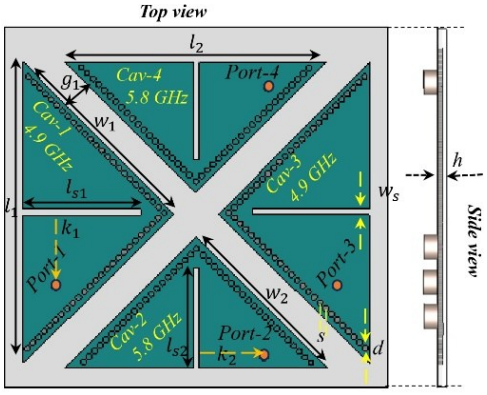

Fig. 1. Proposed 4-port 2×2 MIMO antenna-diplexer yielding two different frequency bands, (l_1 = 19.27, l_2 = 2.5, l_{s1} = 16.5, l_{s2} = 14, g_1 = 4.2, w_1 = 30, w_2 = 26, k_3 = 10, k_2 = 9, s =1.1, d = 0.8, h = 0.787) Unit: *mm.*

II. Configuration and Design Analysis

Fig. 1 illustrates the design configuration sketches of the proposed 2×2 MIMO antenna. The substrate-integrated waveguide (SIW) cavity is constructed using chains of metallic vias that serve as the lateral walls of the planar cavity. These vias effectively form the metallic boundaries of the SIW cavity within the substrate by following guidelines ($d/s \geq 0.5$ and $d/\lambda_o \leq 0.1$) [5–6]. The numerical equations used to calculate the dimensions of for both larger and smaller half-mode cavities are illustrated in equations (1)–(4), respectively [5].

$$f_{L110(HM)} = \frac{c}{2\sqrt{\varepsilon_{reff}}}\sqrt{\left(\frac{m}{w_{1eff}}\right)^2 + \left(\frac{n}{w_1}\right)^2} = \frac{c}{w_{1eff}\sqrt{2\varepsilon_{reff}}} \quad (1)$$

$$f_{H110(HM)} = \frac{c}{2\sqrt{\varepsilon_{reff}}}\sqrt{\left(\frac{m}{w_{2eff}}\right)^2 + \left(\frac{n}{w_2}\right)^2} = \frac{c}{w_{2eff}\sqrt{2\varepsilon_{reff}}} \quad (2)$$

where m =1, n = 1 for the dominant mode of the cavity, f_L = frequency of larger cavity, f_H = frequency of smaller cavity
The relation between physical width and effective width can be defined by using the following equations as follows

$$w_1 = \text{width of } Cav_1 = w_{1eff} + \frac{d^2}{0.95s} \quad (3)$$

$$w_2 = \text{width of } Cav_2 = w_{2eff} + \frac{d^2}{0.95s} \quad (4)$$

d = diameter of the via holes, s = pitch distance between any two consecutives via holes. Fig. 2 outlines the steps to realize the proposed antenna, using scalar and vector E-field distributions to illustrate the design process. Fig. 3 depicts the operating frequency at each stage follows for design evolution. Initially, a full-mode square diamond-shaped cavity with dimensions of 28×28 mm² is excited using a 50Ω characteristic impedance coaxial probe-based feed. The dominant mode of the cavity TE_{110} is achieved around 5.2 GHz. To achieve distinct-size half-mode cavities, the full-mode cavity is bisected along two magnetic walls, *A-A'* and *B-B'*, as shown in Fig. 2(a).

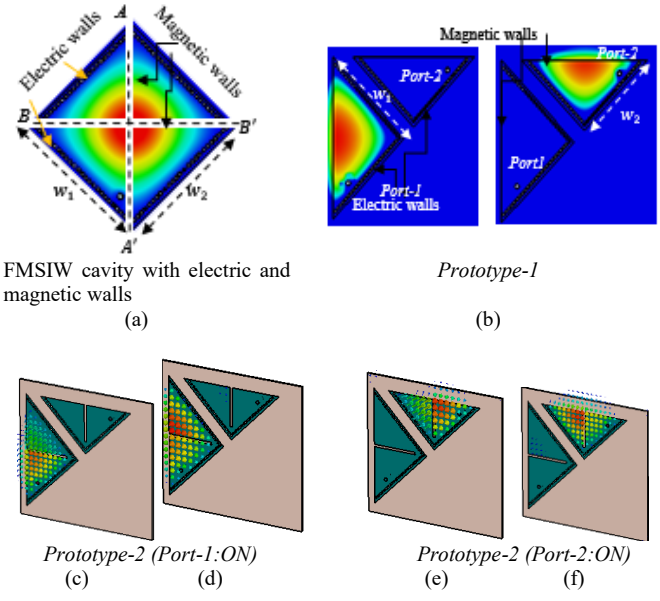

FMSIW cavity with electric and magnetic walls (a)

Prototype-1 (b)

Prototype-2 (Port-1:ON) (c) (d)

Prototype-2 (Port-2:ON) (e) (f)

Fig. 2 (a) Scalar E-field distribution of FMSIW cavity resonating at 5.2 GHz with magnetic- and electric walls, (b)scalar E-field distribution when *Port-1* and *Port-2* are excited separately, (c) and (d) vector E-field distribution after inserting the slot in *Cav1*, (e) and (f) field distribution with inserted slot in *Cav2*.

Both HMSIW cavities of size $w_1 \times w_1$ mm^2 and $w_2 \times w_2$ mm^2 are excited separately and they resonate at 4.9 GHz and 5.8 GHz when *Port-1* and *Port-2* are excited separately, as displayed in Fig. 2(b). By placing two different size cavities orthogonal to each other, high isolation of better than 45 dB is attained, as shown in Fig. 3. In the next step to enlarge the bandwidth, a rectangular slot of length '$0.4\lambda_g$' is engraved at the center of the cavity, where λ_g is the wavelength at the lowermost operating mode i.e. around 4.9 GHz. It can be observed from Fig. 3 that inserting the slot significantly enhances the bandwidth. However, this modification reduces the isolation between the ports by approximately 8 dB. The enhancement in bandwidth can be understood with the help of a vector E-filed plot. When *Port-1* is excited, the slot splits the TE_{110} mode into half-TE_{110} odd mode and half-TE_{110} even mode resonating at 4.85 GHz and 5 GHz, respectively, as shown in Fig. 2(c) and (d), respectively. The odd mode represents equal and opposite fields across the slot, while the even mode represents the same field distribution across the slot. The dimension of the slot plays a key role in the coupling of both modes in proximity. On the other hand, when *Port-2* is excited with 50Ω coaxial probe feed, then both odd-even modes of the *Cav-2* resonate at 5.7 GHz and 5.85 GHz, respectively, as shown in Fig. 2 (e) and (f), respectively.

To achieve a high decoupling while maintaining a compact configuration the distinct resonant frequency radiating element are placed in orthogonal fashion and same resonant frequency elements in parallel arrangement while all HMSIW cavities share the electric walls in proximity. By making this arrangement, the field radiating at the same frequency elements are getting cancelled showing a dip in S_{13} and S_{24} plots at corresponding operating frequencies, as shown in Fig. 4. Thus, with the placement of same frequency elements facing opposite, leads to their radiation pattern showing minimum overlap in far-field. Therefore, isolation better than 30 dB is accomplished between any two ports in a highly compact structure where the inter-element distance is 4.2 mm (≈ $0.09\lambda_g$). In addition, the proposed antenna arrangement maintaining self-diplexing ability. The proposed antenna is designed and analyzed using a 3D CST simulation solver. The optimized antenna parameters

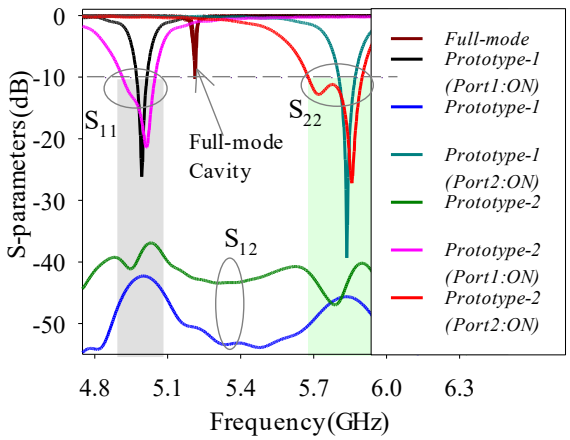

Fig. 3. The S-parameter response for the design evolution from FMSIW cavity - *Prototype-1* and *Prototype-2*.

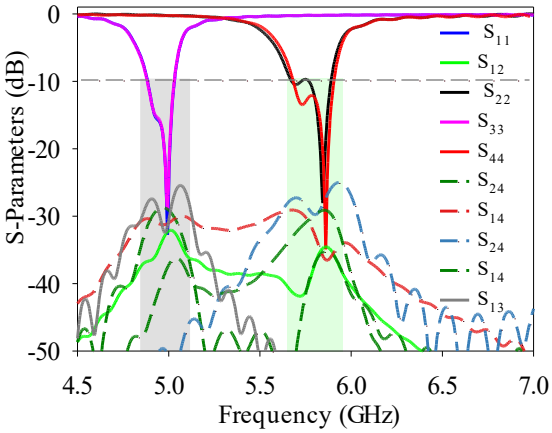

Fig. 4. The S-parameters vs frequency of the proposed 2×2 MIMO antenna-diplexer with 4-ports excited independently.

are symbolized in Fig. 1. The *Cav-1* and *Cav-3* radiates around 4.9 GHz and 5 GHz through the open walls when *Port-1* or *Port-3* is excited individually. Similarly, the *Cav-2* and *Cav-4* radiates around 5.75 GHz and 5.8 GHz, when *Port-2* or *Port-4* is excited, individually.

III. Parametric Analysis and MIMO Parameters

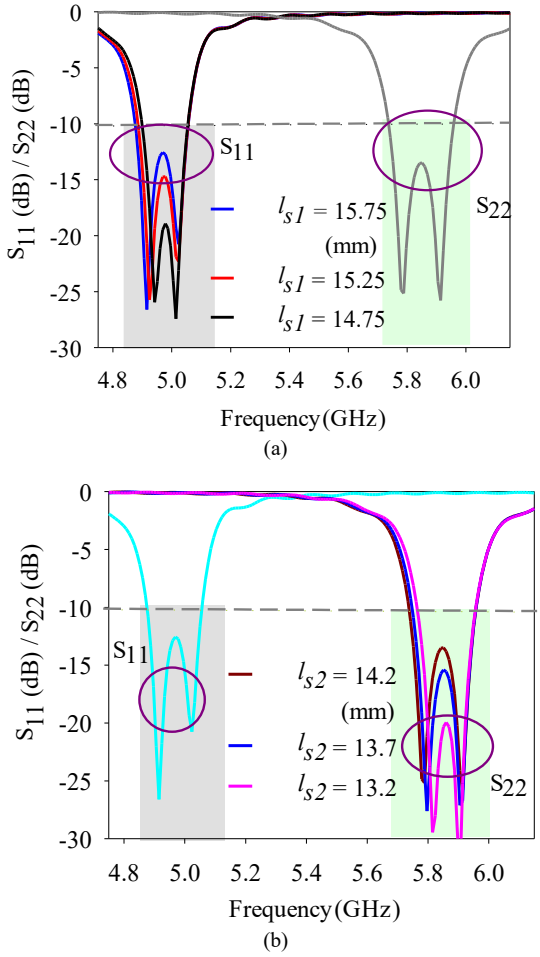

Fig. 5. S-parameters vs frequency with length of the slot (a) when l_{s1} is varied, (b) when l_{s2} is varied.

The proposed design offers great flexibility to tune both operating frequency bands. Optimization of the concerned parameters length of the slots (l_{s1} and l_{s2}) and the position of the slots (k_1 and k_2) is investigated in this section. The variation of S-parameters with change in the parameter l_{s1} when l_{s2} kept constant and vice-versa, displayed in Fig. 5(a) and Fig. 5(b), respectively. As the value of l_{s1} *or* l_{s2} increases individually, the effective radiating aperture area of the HMSIW cavity gets increased to some extent and the resonant frequencies slightly shifts towards the lower frequency. Also, it affects the impedance matching of resonant frequencies in both frequency bands. Similarly, Fig. 6(a) and (b) shows the S-parameter's variation with the port's locations (k_1) and (k_2), from the slots. The k_1/k_2 parameters were varied independently, with one held constant while adjusting other. This variation has significant impact on the coupling between modes in both the lower and upper frequency bands.

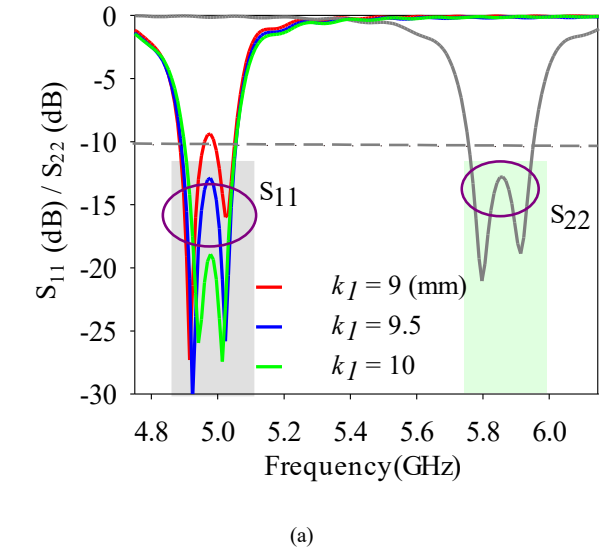

(a)

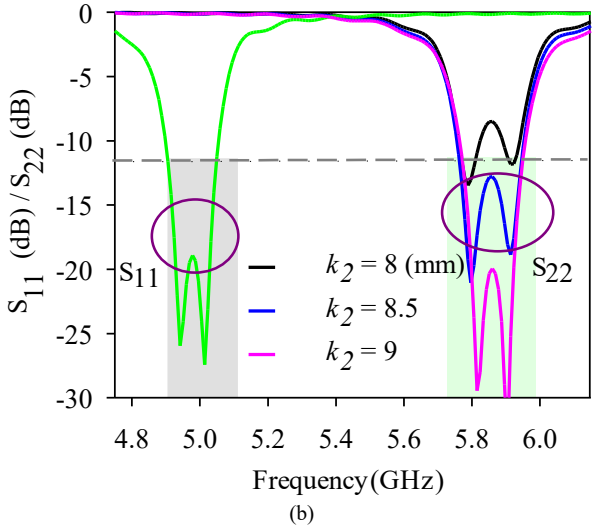

(b)

Fig. 6. S-parameters vs frequency with variation (a) with k_1 (*Port-1* is excited), (b) and k_2 (*Port-2* is excited).

Thus, port location plays an important role in impedance matching of both the modes. Fig. 7 (a) illustrates the variation in reflection coefficients at two ports by varying the gap (g_1) between the cavities. The increasing gap alters the coupling between the two modes, leading to an enhancement in the bandwidth in both upper and lower frequency bands. Fig. 7 (b) features the variation in lower and upper frequency bands with

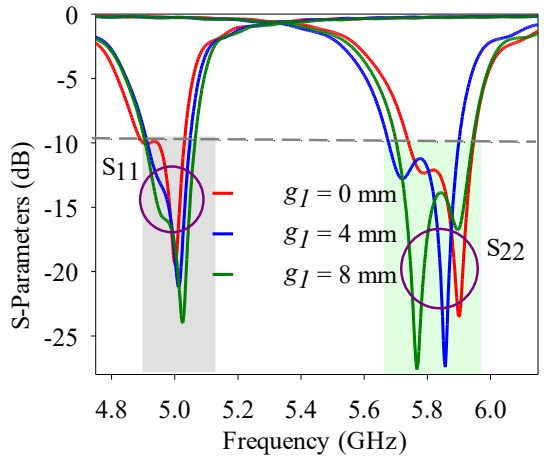

(a)

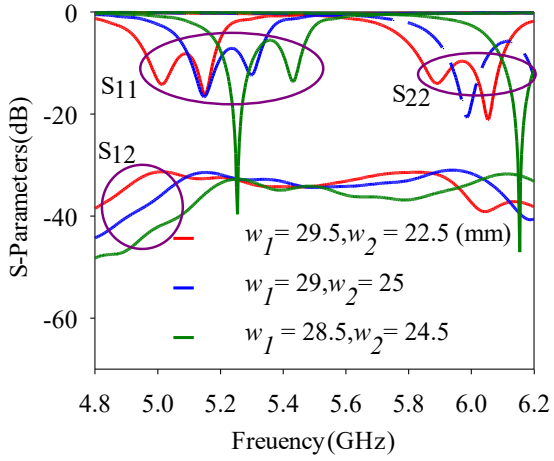

(b)

Fig. 7. S-parameters vs frequency variation, with (a) g_1, (b) w_1 and w_2.

the size of the cavity. The frequency bands shift downward with increase in the size of the cavity due to the increase in the effective aperture area, which provides a longer path for the current to travel. When *Port-1* is turned on, the *Port-2* is terminated with matched load and vice versa.By using the advantages of the common ground plane shared by all the cavities, the overall 2 × 2 elements MIMO antenna contains a compacted area of $1\lambda_g \times 0.9\lambda_g$. To verify the diversity features of the MIMO antenna, an envelope correlation coefficient (ECC) has been extracted from S-parameters, displayed in Fig. 8. The ECC determines the correlation in radiation patterns between two independent antennas. Ideally, it should be zero, however, for most practical applications its value is typically < 0.5. The ECC for the proposed 4-port antenna is < 0.05 in both frequency bands. The ECC has been extracted from S-parameters as well as from far-filed patterns when either *Port-1* and *Port-3* or *Port-2* and *Port-4* are excited simultaneously.

Another diversity parameter is diversity gain (DG) which is used to verify transmission power loss when a diversity mechanism is implemented in the MIMO antenna system. The ideal value of DG should be 10 dB. For the proposed structure this value is achieved is 9.8 dB in lower frequency band when *Port-1*or *Port-3* is excited while it is determined 9.6 dB in upper frequency band when *Port-2* or *Port-4 is* excited [16]. The other crucial parameters are total active reflection coefficient (TARC) and channel capacity loss (CCL) which are plotted in

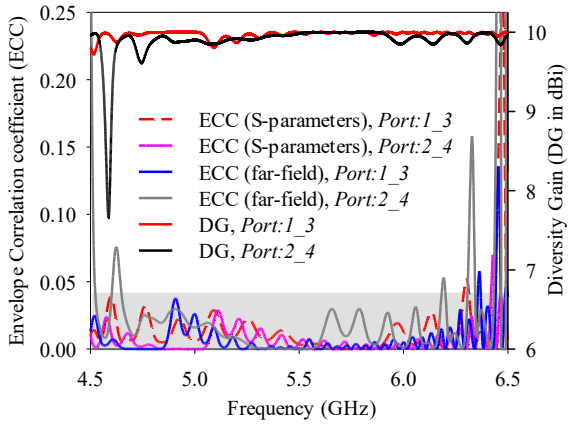

Fig. 8. ECC and DG plots when *Port 1,3* and *Port 2,4* are excited individually.

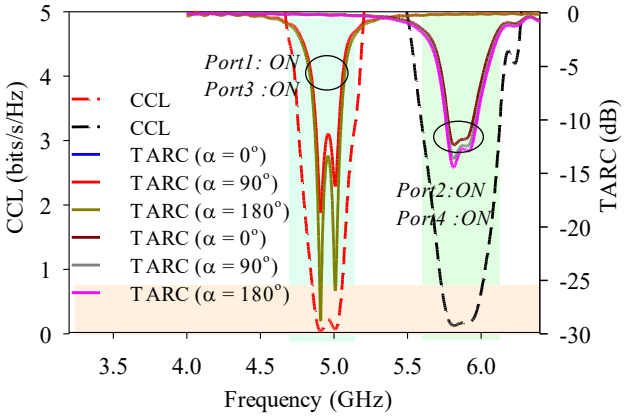

Fig. 9. CCL and TARC vs frequency when *Port 1,3* and *Port 2,4* are excited individually.

Fig. 9 TARC reflects how well each antenna element in the MIMO array is matched to its transmission line and surrounding environment.A low TARC indicates that the antenna elements have minimal reflections while a high TARC value leads to increased reflections and mismatches. For MIMO systems, TARC should ideally be < 0 dB. It can be observed from Fig. 9, that the TARC value is less than -12 dB in operating bands at various angles (α = 0°, 90°, 180°) representing the high matching ability of the antennas [15-16] with its feedlines.

Another crucial parameter for the MIMO antenna is the channel capacity loss, quantified as the difference between the theoretical maximum capacity (in an idealized, noiseless channel) and the actual achievable capacity in a real-world environment. Ideally, it should be zero, however, practically it can be < 0.4 bits/s/Hz. For the proposed antenna the CCL value < 0.1 in both frequency bands of 4.88 GHz–5.03 GHz and 5.72–5.92 GHz, as depicted in Fig. 9. The numerical equations to calculate ECC from S-parameters, MEG, TARC, and CCL are described in [5]–[9]. To validate the proposed design, the MIMO antenna is fabricated and tested in the next section.

IV. Experimental Validations

The proposed self-diplexing MIMO antenna is prototyped on a single layer of Rogers RT Duroid 5880 substrate with a thickness of 1.575 mm. A photograph of the prototyped with its top plane and bottom plane are displayed in Fig. 10 (a) and (b), respectively.

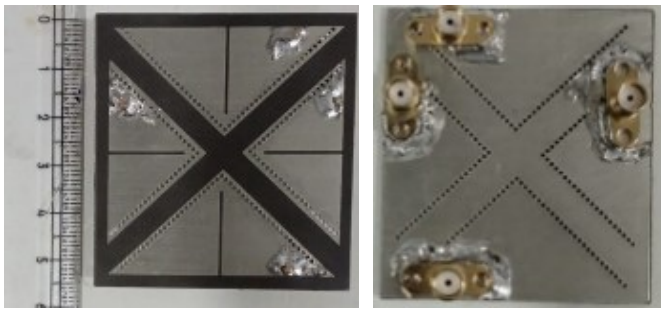

(a) (b)

Fig. 10. Photograph of the fabricated prototype (a) front view (b) bottom view.

The proposed prototype is experimentally verified and both simulated as well as measured responses are compared in Fig. 11. When *Port-1* is excited, the simulated results cover the bandwidth (4.87–5.05 GHz, 180 MHz) while the measured results show (4.87–5.02 GHz, 150 MHz) in the lower frequency band. On the other hand, when *Port-2* is excited, the simulated results cover the bandwidth (5.71–5.92 GHz, 210 MHz) while the measured results show (5.64–5.89 GHz, 250 MHz) in the upper-frequency band. The proposed antenna demonstrates the measured fractional bandwidth of 3.1 % in the lower frequency band and 4.3% in the upper frequency band.

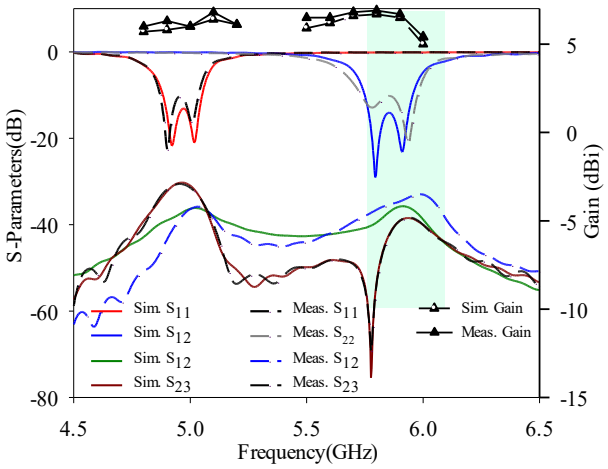

Fig. 11. Simulated and measured results: S-parameters and gain vs frequency.

The simulated / measured gain is observed in the range of 4.79–5.1 dBi / 4.8–5.2 dBi in the lower frequency band when *Port-1* is ON while 5.59–5.75 dBi / 5.59–5.86 dBi in the upper frequency band when *Port-2* is ON and rest of the ports are

TABLE I
PERFORMANCE THE COMPARISON OF PROPOSED ANTENNA WITH OTHER EXISTING DESIGNS

Parameters	Operating Frequency, f_r (GHz)	Antenna Topology	MIMO Antenna	Peak Gain in operating frequency bands (dBi)	Feeding Technique / No. of layers	Minimum Isolation between two elements (dB)	Total Size in (Electrical length)	No. of elements used in antenna
[9]	28/38	Monopole	Yes	6.9	Microstrip / Single	30	2.6 λ_g × 2.6 λ_g	1×1
[11]	2.63	Parasitic strip	Yes	5.5	Coaxial/ Single	17	1.5 λ_g × 1.5 λ_g	2×2
[12]	2.45/3.5	T-Slot	Yes	2.4/3.4	Coaxial/double	19	0.7 λ_g ×1.7 λ_g	1×1
[13]	2.45	SICBS	Yes	7	Coaxial / 25	20	≈1.8 λ_g×1.8 λ_g	2×2
[15]	3.4/4.3	HMSIW	Yes	5.3/6.7	Coaxial/ Single	23	1 λ_g × 1.2 λ_g	2×2
[16]	5	HMSIW	Yes	5.6	Single	25	1.6 λ_g ×1.6 λ_g	2×2
[17]	2.4/5.5	SIW	Yes	2.9/5	Coaxial/ Single	20	0.8 λ_g × 0.9 λ_g	1×1
[18]	3.5	SIW	Yes	4.9	Coaxial / N.A.	14	0.8 λ_g×1.6 λ_g	2×2
[19]	5.2 / 5.8	SD-HMSIW	Yes	5.26 / 4.94	Microstrip / Single	21	0.4 λ_g × 0.4 λ_g	1×1
[20]	6.2 / 7.75	SIW	No	NA	Microstrip / Single	22	0.88λ_g×0.88 λ_g	1×1
[21]	12/14	SIW	No	NA	Microstrip / Single	19	1.4λ_g × 1.3λ_g	2×2
Here	4.9 / 5.8	HMSIW	Yes	5.9/5.2	Coaxial/ Single	30	1.0 λ_g × 0.9 λ_g	2×2

[λ_g is the guide wavelength at 4.9 GHz]

terminated with matched loads. The transmission coefficients S_{12} and S_{23}, which indicate the isolation between *Port-1* and *Port-2*, as well as between *Port-2* and *Port-3*, are tested and compared with simulation results. Both the simulated and measured data show that the minimum isolation between any two ports of the antenna exceeds 30 dB. The slight discrepancies observed in in the simulation and measurement results for both reflection coefficients (S_{11}, S_{22}) and transmission coefficient (S_{12}, S_{23}) plots, as in the simulation studies, the metallic plane is modelled as a Perfect Electric Conductor (PEC), which is an idealized material with zero electrical resistance and infinite conductivity. However, in the fabricated prototype, copper is used, which has a finite conductivity of 5.8×10^7 S/m. The simulated and measured co-polarized and cross-polarized radiation patterns at two principal cut-planes, $\phi = 0°$ (YZ-plane) and $\phi = 90°$ (XZ-plane), at the resonant frequencies, are plotted in Fig. 12.

The radiation patterns at each plane are found stable and unidirectional, with a measured front-to-back ratio (FTBR) greater than 10 dB in both frequency bands. The co-polarized to cross-polarized level exceeds 17 dB in the YZ-plane and more than 11 dB in the XZ-plane for both the upper and lower frequency bands in the direction of maximum radiation.

The proposed design demonstrates an adequate front-to-back ratio (FTBR) and radiates maximally in the boresight direction, thanks to the cavity-backed structure. It is simple and planar topology makes it suitable for realizing a compact and integrated system. To underscore the contribution of the proposed work, a comparative study with previously reported works is presented in Table.1. The proposed design offers superior isolation compared to other existing 4-port antennas while maintaining a relatively smaller circuitry size and achieving higher gain in both frequency bands. The proposed antenna structure is realized on a single layer, ensuring a compact profile with self-diplexing MIMO capability. The proposed antenna is the modifications of the previous design in terms of cavity shapes as illustrated in [15]. By opting diamond-shaped SIW cavities, the proposed antenna offers a better isolation of around 8 dB than the previous antenna. The proposed MIMO antenna configuration achieves an efficiency greater than 94% across both operating bands which is 16% higher than the 80% efficiency of the previous design. This 4-port MIMO antenna enhances channel capacity 2 times as compared to a 2-port self-diplexing antenna, which is crucial for enhancing channel capacity significantly. It can be observed that the proposed design owns better isolation than any other existing 4-port antenna with relatively smaller circuitry in size with relatively higher gain value in both of the frequency bands. The proposed single-layer geometry maintains a compact profile with self-diplexing MIMO capability. The proposed antenna features self-diplexing capabilities, allowing for simultaneous operation of its transceivers, combined with MIMO technology which enhances both data rates and communication reliability.

V. CONCLUSION

This article presents a compact 4-port self-diplexing MIMO antenna designed for WLAN at 5 GHz and ISM band at 5.8 GHz. By leveraging the symmetrical nature of the TE_{110} mode and utilizing HMSIW techniques, the design achieves a 50% size reduction. Radiating elements positioned out of phase effectively cancel field coupling, resulting in isolation exceeding 30 dB between any two ports in a compact space of either parallel elements or orthogonal elements. The design shows that MIMO performance metrics, including ECC, MEG, CCL, and TARC, are within satisfactory limits. The proposed

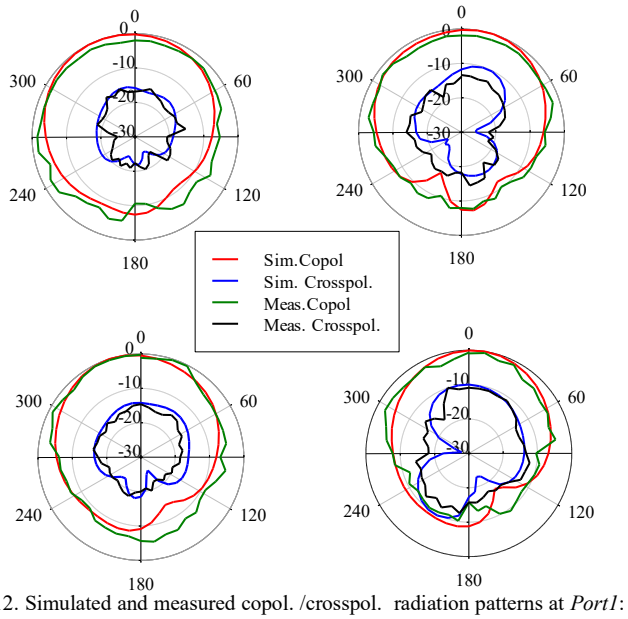

Fig. 12. Simulated and measured copol. /crosspol. radiation patterns at *Port1*: ON (a) ϕ = 0º at 5 GHz, (b) ϕ = 90º at 5 GHz while *Port2*: ON (c) ϕ = 0º at 5.8 GHz, (d) ϕ = 90º at 5.8 GHz.

antenna features a simple, low-profile configuration with self-diplexing capabilities, offering dual channel capacity in both frequency bands. Its compact design, reliable communication, and superior radiation properties make it ideal for dense wireless communication networks. Furthermore, the proposed antenna boasts a simple and scalable design, making it adaptable to higher frequency bands and suitable for future advancements in massive MIMO technology for 5G mmWave networks aimed at high-speed data transmission. Additionally, its self-diplexing capability and high isolation make it an ideal candidate for full-duplex wireless systems, enabling simultaneous transmission and reception with minimal interference.

REFERENCES

[1] M. A. Jensen and J. W. Wallace, “A review of antennas and propagation for MIMO wireless communications,” *IEEE Trans. Antennas Propag*., vol. 52, no. 11, pp. 2810–2824, 2004, doi: 10.1109/TAP.2004.835272.

[2] D. Gesbert, M. Kountouris, R. W. Heath, Jr., C.-B. Chae, and T. Sälzer, "Shifting the MIMO Paradigm: From Single User to Multiuser Communications," *IEEE Signal Process. Mag.,* vol. 24, pp. 36-46, 2007, doi: 10.1109/MSP.2007.904815.

[3] Kumar, D. Chaturvedi, A. A. Khan “Bandwidth-Improved HMSIW Resonator based Filtennas for Single/Dual Channel Network,” IEEE Indian Conference on Antennas and Propagation (InCAP), pp. 502–505, 2021, doi: 10.1109InCAP52216.2021.9726509.

[4] M. S. Sharawi, “Printed multi-band MIMO antenna systems and their performance metrics,” *IEEE Antennas Propag. Mag.,* vol. 55, no. 5, pp. 218–232, 2013, doi: 10.1109/MAP.2013.6735522.

[5] D. Chaturvedi, P. Jadhav, A. A. Althuwayb, and K Aliqab, “A Compact 2-Port QMSIW Cavity-Backed MIMO Antenna with Varied Frequencies using CSRR-Slot Angles for WBAN Application,” *IEEE Access*, vol. 12, pp. 100506–100514, 2024, doi: 10.1109/ACCESS.2024.3425520.

[6] K. Pandey, N. K. Sahu, R. K. Gangwar and R. K. Chaudhary, "SIW-Cavity-Backed Wideband Circularly Polarized Antenna Using Modified Split-Ring Slot as a Radiator for mm-Wave IoT Applications," in *IEEE Internet of Things J.*, vol. 11, no. 7, pp. 11793-11799, 2024, doi: 10.1109/JIOT.2023.3332169.

[7] K. Pandey, R. K. Gangwar and R. K. Chaudhary, "A Compact SD-QMSIW-Based Self-Diplexing MIMO Antenna Using Two Modified L-Shaped Slots as Radiators for IoT Applications," *IEEE Internet Things J.*, vol. 12, no. 3, pp. 2385 – 2394, 2024, doi: 10.1109/JIOT.2024.3464590.

[8] D. Chaturvedi, A. Kumar, “A QMSIW cavity-backed self-diplexing antenna with tunable resonant frequency using CSRR slot,” *IEEE Antennas Wirel. Propag. Lett*, vol. 23, no. 1, pp. 259–263, 2023, , doi: 10.1109/LAWP.2023.3323008.

[9] W. A. Ali, A. A. Ibrahim, and A.E. Ahmed, “Dual-Band Millimeter Wave 2×2 MIMO Slot Antenna with Low Mutual Coupling for 5G Networks,” *Wirel. Pers. Commun*., vol. 129, pp. 2959–12976, 2023, https://doi.org/10.1007/s11277-023-10267-w.

[10] M. Ikram, R. et al, "Compact 4-element MIMO antenna with isolation enhancement for 4G LTE terminals," *IEEE Int. Symp. Antennas Propag. (APSURSI),* 2016, doi: 10.1109/APS.2016.7695976.

[11] K. Ding, C. Gao, D. Qu, and Q. Yin, ‘‘Compact broadband MIMO antenna with parasitic strip,’’ *IEEE Antennas Wirel. Propag. Lett*., vol. 16, pp. 2349–2353, 2017, doi: 10.1109/LAWP.2017.2718035.

[12] S. Zhang, B. K. Lau, Y. Tan, Z. Ying, and S. He, “Mutual coupling reduction of two PIFAs with a T-shape slot impedance transformer for MIMO mobile terminals,” *IEEE Trans. Ant. Propag*., vol. 60, no. 3, pp. 1521-31, 2011, doi: 10.1109/TAP.2011.2180329.

[13] G. Zhai, Z. N. Chen, and X. Qing, “Enhanced isolation of a closely spaced four-element MIMO antenna system using metamaterial mushroom,” *IEEE Trans. Ant. Propag*, vol. 63, no. 8, pp. 3362-3370, 2015, doi: 10.1109/TAP.2015.2434403.

[14] F. Liu, J. Guo, L. Zhao, G. L. Huang, Y. Li, and Y. Yin “Ceramic superstrate-based decoupling method for two closely packed antennas with cross-polarization suppression,” *IEEE Trans. Ant. Propag*., vol. 69, no. 3, pp. 1751-1756, 2021, doi: 10.1109/TAP.2020.3016388.

[15] Pramodini, D. Chaturvedi, and G. Rana, “Design and Investigation of Dual-Band 2×2 Elements MIMO Antenna-Diplexer Based on Half-Mode SIW,” *IEEE Access*, vol. 10, pp. 79272–79280, 2022, doi: 10.1109/ACCESS.2022.3193253.

[16] A. Elobied, X. X. Yang, T. Lou, and S. Gao, “Compact 2× 2 MIMO antenna with low mutual coupling based on half mode substrate integrated waveguide,” IEEE *Trans. Ant. Propag*., vol. 69, no. 5, pp. 2975-2980, 2020, doi: 10.1109/TAP.2020.3028250.

[17] S. Yan, P. J. Soh, and G. A. E. Vandenbosch, “Dual-Band Textile MIMO Antenna Based on Substrate-Integrated Waveguide (SIW) Technology,” *IEEE Trans. Antennas Propag*., vol. 63, no. 11, pp. 4640–4647, 2015, doi: 10.1109/TAP.2015.2477094.

[18] Niu, and J. H., Tan “Compact four-element MIMO antenna system based on substrate-integrated-waveguide cavities,” *Prog. Electromagn. Res. Lett*., 88, pp.143-149, 2020, doi:10.2528/PIERL19102701.

[19] K. Pandey, R. K. Gangwar, and R. K. Chaudhary, “A compact frog-shaped self-diplexed MIMO antenna with SD-HMSIW technique for WLAN applications,” IEEE Trans. Antennas Propag., 2025, doi:10.1109/TAP.2025.3548684

[20] N. C. Pradhan, S. S. Karthikeyan, R. K. Barik, and Q. S. Cheng, “A novel compact diplexer employing substrate integrated waveguide loaded by triangular slots for C-band application,” *J. Electromagn. Waves Appl.,* vol.36, no. 6, pp. 830–842, 2022, https://doi.org/10.1080/09205071.2021.1987991

[21] K. Zhou, C. Zhou, and W. Wu, “Compact planar substrate-integrated waveguide diplexers with wide-stopband

characteristics," *Int. J. RF Microw. Comput-Aid. Eng.*, vol. 30, no. 6, pp. e22179, 2020, https://doi.org/10.1002/mmce.22179.

Divya Chaturvedi was born in Kanpur, India. She received her B. Tech. degree in Electronics and Communication Engineering from Uttar Pradesh Technical University, India in 2011 and the M. Tech. degree in Electronics Engineering from Pondicherry Central University, India in 2015. She has obtained her Ph.D. degree in the area of Substrate-Integrated Waveguide based cavity-backed antenna at National Institute of Technology, Tiruchirappalli in 2019. Currently, she is working as an Assistant Prof. at Dept. of Electronics and Communication Engineering, IIIT Pune, Maharashtra. She is an active researcher in substrate-integrated waveguide antennas, filters, beam forming antennas, variable antennas and biological effects ofradiation on human body. She has published several papers on SIW self-multiplexing antennas in IEEE TAP, IEEE AWPL, RFCAD, IET-MAP journals. She is a senior member of IEEE APS, MTT, WiE.

Tiruganesh Lanka born in Challapalli, India. He received his B. Tech degree in Electronics and Communication Engineering from Jawaharlal Nehru Technological University, (JNTU) Kakinada, India in2009 and the M. Tech degree in Computer and Communication Engineering from the University College of Engineering, J.N.T.U.K, Kakinada, in 2011. Currently, he is pursuing his Ph.D. at Dept of Electronicsand Communication Engineering, at SRM University -AP, Amaravathi, India.

Arvind Kumar received his Ph. D in Microwave and RF in the Department of Electronics and Communication Engineering at the National Institute of Technology Tiruchirappalli, India, in 2019. He also completed a Master's degree (M. Tech.) with a specialization in Electronics from Pondicherry Central University and obtained his Bachelor's degree (B. Tech) in Electronics and Communication Engineering from Govt. engineering College Ajmer, affiliated with Rajasthan Technical University, Kota Rajasthan in 2012. He has achieved notable recognition as one of the Top 2% scientists in the World (all fields).: according to a survey conducted by Stanford University. This recognition is based on factors such as citations, h-index, and co-authorship adjusted h-index, for three consecutive years, spanning 2020,2021 and 2022. He has published several papers on SIW self-multiplexing antennas in IEEE TAP, IEEE AWPL, IET-MAP journals. He is a senior member of IEEE APS, MTT.